Analytical and Bioanalytical Chemistry
https://doi.org/10.1007/s00216-020-02621-9

RESEARCH PAPER

Creation of an electrokinetic characterization library for the detection and identification of biological cells

Adriana Coll De Peña[1,2] · Abbi Miller[1] · Cody J. Lentz[1] · Nicole Hill[1] · Anutthaman Parthasarathy[2] · André O. Hudson[2] · Blanca H. Lapizco-Encinas[1]

Received: 13 February 2020 / Revised: 19 March 2020 / Accepted: 26 March 2020

Abstract

The rising concern over drug-resistant microorganisms has increased the need for rapid and portable detection systems. However, the traditional methods for the analysis of microorganisms can be both resource and time intensive. This contribution presents an alternative approach for the characterization of microorganisms using a microscale electrokinetic technique. The present study aims to develop and validate a library with a novel parameter referred to as the electrokinetic equilibrium condition for each strain, which will allow for fast identification of the studied bacterial and yeast cells in electrokinetic (EK) microfluidic devices. To create the library, experiments with six organisms of interest were conducted using insulator-based EK devices with circle-shaped posts. The organisms included one yeast strain, *Saccharomyces cerevisiae*; one salmonella strain, *Salmonella enterica*; two species from the same genus, *Bacillus cereus* and *Bacillus subtilis*; and two *Escherichia coli* strains. The results from these experiments were then analyzed with a mathematical model in COMSOL Multiphysics®, which yielded the electrokinetic equilibrium condition for each distinct strain. Lastly, to validate the applicability EK library, the COMSOL model was used to estimate the trapping conditions needed in a device with oval-shaped posts for each organism, and these values were then compared with experimentally obtained values. The results suggest the library can be used to estimate trapping voltages with a maximum relative error of 12%. While the proposed electrokinetic technique is still a novel approach and the analysis of additional microorganisms would be needed to expand the library, this contribution further supports the potential of microscale electrokinetics as a technique for the rapid and robust characterization of microbes.

Keywords Biological cells · Dielectrophoresis · Electrophoresis · Electrokinetics · Microfluidics · Microorganisms

Introduction

While it is difficult to determine an exact value, scientists seem to agree that there are over 10^7 distinct species of bacteria that exist [1, 2]. With rising concerns over antibacterial resistance, the genetic diversity that allows bacteria to thrive under varied conditions becomes of increasing interest as these genes can be exploited for human applications in the pharmaceutical and agricultural sectors. To emphasize their diversity, it must be noted that there are species that can tolerate and thrive in conditions with a pH as low as 0 or as high as 12.8, temperatures as low as − 20 °C or as high as 122 °C, and pressures of up to 110 MPa [3]. Moreover, their well-characterized genetic exchange abilities make them a great model to analyze and characterize genes from other organisms. Similar to bacteria, yeast is also a naturally occurring and prevalent microbe in the environment with great medical, agricultural, and gastronomical implications. Despite the

Published in the topical collection *Bioanalytics and Higher Order Electrokinetics* with guest editors Mark A. Hayes and Federica Caselli.

Electronic supplementary material The online version of this article (https://doi.org/10.1007/s00216-020-02621-9) contains supplementary material, which is available to authorized users.

✉ André O. Hudson
aohsbi@rit.edu

✉ Blanca H. Lapizco-Encinas
bhlbme@rit.edu

[1] Microscale Bioseparations Laboratory and Biomedical Engineering Department, Rochester Institute of Technology, Institute Hall (Bldg. 73), 160 Lomb Memorial Drive, Rochester, NY 14623-5604, USA

[2] Thomas H. Gosnell School of Life Sciences, Rochester Institute of Technology, Gosnell Hall (Bldg. 8), 85 Lomb Memorial Drive, Rochester, NY 14623, USA

Published online: 22 April 2020

extensive knowledge in traditional microbiological methods, a major bottleneck when working with samples from the environment is their heavy resource requirements. Usually, common identification processes require hours to days of work with long incubation periods due to use of differential media, nucleic acid tests, dye pour-plate auxanographic tests, Gram stains, antibody tests, antigen tests, etc. [4, 5]. However, under certain circumstances, the time required for the identification/detection is critical. In addition, some methods can significantly decrease cell viability precluding the sample from being used for further analysis. This loss of sample quantity and quality is a major concern when working with small volumes or if several tests are necessary. These limitations were the motivation behind exploring an alternative method for the analysis of biological samples that would reduce the analysis time by streamlining the analysis process to facilitate identification and potential purification of the sample.

Microfluidics is a field that specializes in high-resolution and purification assays that has reshaped how bioanalytical assessments are performed [6]. When a solid surface is in contact with an aqueous solution, the surface will generally acquire an electrical charge due to the ionization and adsorption of ions on the surface [7, 8]. To balance the surface charge, a thin layer of highly concentrated ions is formed above the surface, creating what is known as the electrical double layer (EDL). Electrokinetics are electric field–driven techniques that depend on the EDL and have become one of the leading pillars in microfluidics due to their flexibility and simplicity in application, having been successfully used for both biomedical and clinical analyses [9–11]. Dielectrophoresis (DEP), the migration of particles due to the polarization effects of a non-homogeneous electric field, has shown great potential in the purification and enrichment of biological particles [12–17]. Moreover, since the insulating structures used to disturb the electric fields generally transverse the entire height of the microchannel, it affects all the particles within the system, creating a 3D effect [18]. Unlike linear electrophoresis ($EP^{(1)}$), which separates particles based on charge, DEP has been reported as a more robust separation method with greater flexibility as it exploits the polarization effects of particles, allowing the technique to be used on neutral and charged particles with both AC and DC electric potentials [19–22]. However, as previously suggested by several research groups, this study suggests that at higher electric fields, results previously attributed to DEP may actually be the result of electrophoresis of the second kind ($EP^{(3)}$) [23–27]. Therefore, DEP-related studies, and in particular iDEP-related studies, will be discussed in an attempt to provide background for this contribution.

In closer examination of previous works in this field, much literature has contributed to introducing biological samples in DEP systems. Specifically, the work done by Elitas et al. [28] found DEP as a viable technique for characterizing live bacterial cell cultures and their use in point-of-care diagnostics as well as applications for monitoring bacterial infections. A study done by Hilton et al. [29] showed that different bacterial strains can be manipulated using DEP with DC electric potentials. Hilton et al. also used this technique to address the issue of the limited ability to interpret the significance of the variation between two cell populations. Syed et al. [30] applied AC DEP techniques to capture *Escherichia coli* cells. Their research proved the intrinsic dielectric properties of photogenic bacteria could be used to effectively detect, capture, and release culture samples of small volumes. Another study done by Seyedi et al. [31] showed these theories could also be applied to protein particles, illustrating the applicability with nanobiological particles. Their work examined the electrokinetic behavior of protein particles under manipulation by dielectrophoresis. In particular, they performed molecular dynamics simulations of the protein cytochrome *c* in solution to evaluate the variance of its refractive index and dipole moment, which directly affects the effective polarity of the protein. Coll De Peña et al. [15] reported that insulator-based DEP (iDEP) systems could successfully characterize and separate bacteriophage viruses while retaining viability. Furthermore, adding to the parameter introduced by Mohammadi et al. [32] and Crowther et al. [33], Coll De Peña et al. [15] explored the use and application of the parameter trapping value (*Tv*) as a standard for characterizing different species. In regard to the retention of viability of the samples being used, LaLonde et al. [14] addressed how the magnitude of an applied electric potential, exposure time, and suspending medium osmolality affect cell viability in iDEP systems. These findings were critical for the validation of the operating conditions of iDEP devices when using samples containing biological cells. Wang et al. [34] studied the relationship between the polarizability of microbial cell envelope and electrochemical activity by studying *Geobacter sulfurreducens*, *Shewanella oneidensis*, and *Escherichia coli* wild-type and mutant strains that had modifications in their genes of interest. Rather than using traditional extracellular electron transfer phenotyping techniques to characterize their microorganisms, which require large sample volumes and can require complex experimental procedures, they used microfluidic DEP, which allowed them to show a strong correlation between bacterial cell extracellular electron transfer and surface polarizability. Other earlier contributions to DEP-based bacteria and yeast studies were performed during the late 1990s and early 2000s, showing a constantly increasing interest in the dielectrophoretic manipulation of biological cells [35–40].

The studies discussed above reflect upon the current state and latest advancements in the electrokinetic (EK) characterization and manipulation of biological particles, in particular bacterial and yeast cells. However, despite the vast experiments that have been conducted to analyze, enrich, and separate microorganisms, the potential of creating a functional and

translational library with the unique electrokinetic signature of microorganisms has yet to be explored. There is currently a shortage of techniques that would allow for rapid characterization of cells with limited effect on viability and whose parameter can be used in homologous systems, in particular when limited volumes are available. Thus, this contribution introduces the idea of such a library and supports it with experiments in a homologous system. The original electrokinetic behavior that is specific to the system in which the experiments are run would be obtained experimentally with devices containing an array of circle-shaped insulating posts (Fig. 1a, b), and used as one of the inputs for our 2D COMSOL Multiphysics® mathematical model to estimate the electrokinetic equilibrium condition (E_{EEC}) of each strain (see Eq. (11)). The E_{EEC} will then be used to extrapolate the conditions required to identify the cells of interest in the homologous system (oval-shaped post device, Fig. 1c). The parameter E_{EEC} integrates the main EK phenomena acting on the cells (electrophoresis of the 1st and 2nd kind and electroosmosis) and will be used for the optimization of EK systems aiming to separate and enrich samples while keeping viability retention a priority.

Theory and mathematical modeling

Theory

At low electric field magnitudes, the migration of particles within a microchannel is dictated by linear electrokinetics, which is the superposition of linear electrophoresis $EP^{(1)}$ and electroosmosis (EO). The expressions for the EO and $EP^{(1)}$ velocities are given by [41]:

$$\mathbf{v}_{EP}^{(1)} = \mu_{EP}^{(1)}\mathbf{E} \tag{1}$$

$$\mathbf{v}_{EO} = \mu_{EO}\mathbf{E} \tag{2}$$

where $\mathbf{v}_{EP}^{(1)}$ is the linear $EP^{(1)}$ velocity, $\mathbf{v}_{EO}$ is the EO velocity, $\mathbf{E}$ is the electric field, and $\mu_{EP}^{(1)}$ and μ_{EO} are the linear electrophoretic and electroosmotic mobilities, respectively. These mobilities depend on the particle zeta potential (ζ_P) and the zeta potential of the channel wall (ζ_W), respectively, as well as on media viscosity (η), and media permittivity (ε_m):

$$\mu_{EP}^{(1)} = \frac{\varepsilon_m \zeta_P}{\eta} \tag{3}$$

$$\mu_{EO} = -\frac{\varepsilon_m \zeta_W}{\eta} \tag{4}$$

At higher electric fields, which are relative to the EK properties of the particle, an additional non-linear EP phenomenon becomes more noticeable and affects particle migration [42]. This effect is called electrophoresis of the second kind ($EP^{(3)}$), and it depends on the cube of the electric field as it has been reported by several research groups [23–27]. For the present study, the models derived by Dukhin [23] and the Yariv group [24, 26] could apply, since under our conditions, the voltage drop across a particle is comparable or larger than the thermal voltage (25 mV). The voltage drops, estimated as the electric field times the particle radius ($\mathbf{E} \cdot r_p$), for the bacterial and yeast cells in this study ranged from 69 to 268 mV. These three models [23, 24, 26] require the addition of a non-linear velocity term proportional to the cubic power of the electric field strength. Shilov et al. [42] reported a study on non-linear EP, where they distinguished between linear EP ($EP^{(1)}$) and non-linear EP ($EP^{(3)}$). They reported that as soon as the electric field strength is increased, the non-linear phenomena that depend on $\mathbf{E}$ start playing a more significant effect on particle migration due to EP, illustrating a clear non-linear dependence of $\mathbf{v}_{EP}$ on $\mathbf{E}$. They explained that the effect of this non-linear dependence appears higher than first-order terms in the

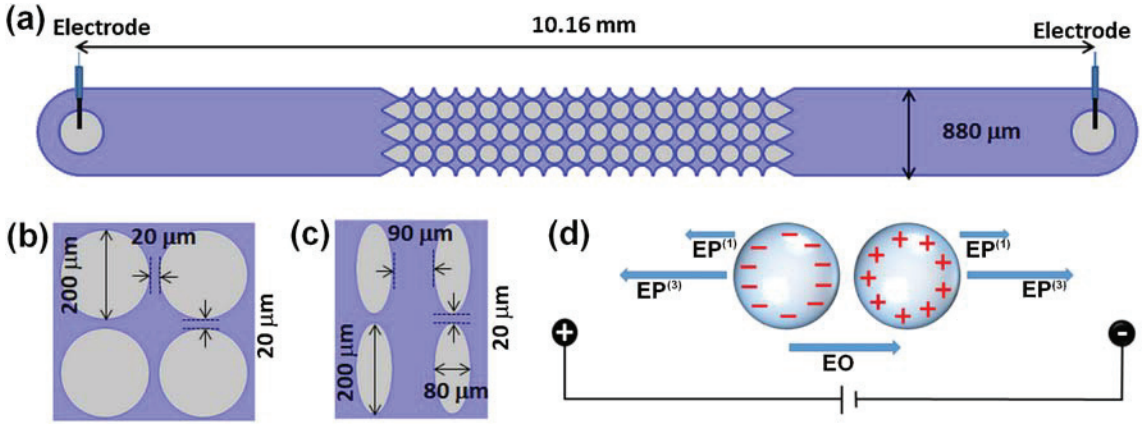

Fig. 1 Schematic illustration of one of the insulator-based microchannel designs. **a** Full channel for design Circle-200-220 depicting the post array and inlet and outlet reservoirs. For the two designs analyzed in this study, an illustration of four insulating posts with dimensions is included: **b** Circle-200-220, **c** Oval-200-220&80-170. Design names illustrate post size followed by post center-to-center spacing lateral and longitudinal dimensions. **d** Illustration of the forces acting on particles with negative and positive charges, respectively, when exposed to an electric field

expansion of $\mathbf{v}_{EP}$ in power of $\mathbf{E}$ and that $\mathbf{v}_{EP}$ is an odd function of $\mathbf{E}$, and therefore, the corresponding even powers are absent (i.e., there is not a term with dependence on $\mathbf{E}^2$). This behavior arises from the fact that the direction of $\mathbf{v}_{EP}$ depends on the direction of $\mathbf{E}$ and that changing the sign (direction) of $\mathbf{E}$ without changing its absolute value, would change the sign of $\mathbf{v}_{EP}$. Thus, the first two terms in the expansion of $\mathbf{v}_{EP}$ with respect to $\mathbf{E}$ are [42]:

$$\mathbf{v}_{EP} = \mu_{EP}^{(1)}\mathbf{E} + \mu_{EP}^{(3)}|\mathbf{E}|^3\mathbf{i} \tag{5}$$

where both $\mu_{EP}^{(1)}$ and $\mu_{EP}^{(3)}$ are field-independent and $\mu_{EP}^{(3)}$ is the electrophoretic mobility of the second kind. Consequently, the expression for the *EP* velocity of the second kind ($\mathbf{v}_{EP}^{(3)}$), which is proportional to the cubic power of the electric field strength, is defined as [42]:

$$\mathbf{v}_{EP}^{(3)} = \mu_{EP}^{(3)}|\mathbf{E}|^3\mathbf{i} \tag{6}$$

where $\mathbf{i}$ is a unit vector in the applied electric field direction [24]; the use of this vector satisfies the vector nature of $\mathbf{v}_{EP}^{(3)}$. A second non-linear phenomenon to consider that has been extensively studied is dielectrophoresis (DEP) [19, 20], which is defined as particle migration as a function of polarization effects in the presence a non-homogeneous electric field. The DEP velocity of a particle is defined as:

$$\mathbf{v}_{DEP} = \mu_{DEP}\nabla E^2 \tag{7}$$

where μ_{DEP} is the DEP mobility. Considering all four phenomena mentioned above, the overall expression for particle velocity within a microchannel (Fig. 1a) becomes:

$$\mathbf{v}_p = \mathbf{v}_{EO} + \mathbf{v}_{EP}^{(1)} + \mathbf{v}_{EP}^{(3)} + \mathbf{v}_{DEP} \tag{8}$$

However, from our own estimations of the relative contributions of these four phenomena to the overall particle velocity (see Electronic Supplementary Material (ESM) Table S1), it was found that the dielectrophoretic velocity ($\mathbf{v}_{DEP}$) magnitude was 0.89 to 5.85% of the $EP^{(3)}$ velocity. Considering this, by neglecting the contribution of $\mathbf{v}_{DEP}$, the particle velocity can be simplified as follows:

$$\mathbf{v}_p = \mathbf{v}_{EO} + \mathbf{v}_{EP}^{(1)} + \mathbf{v}_{EP}^{(3)} = \mu_{EO}\mathbf{E} + \mu_{EP}^{(1)}\mathbf{E} + \mu_{EP}^{(3)}|\mathbf{E}|^3\mathbf{i} \tag{9}$$

The majority of biological particles, such as cells, possess a negative charge. If we consider a microchannel with a negative wall zeta potential, like PDMS, the direction of the *EO* flow would be opposite to that of the two *EP* contributions ($EP^{(1)}$ and $EP^{(3)}$) for negatively charged particle. This means there is a particular electric field condition under which the overall particle velocity is 0; i.e., the particle becomes "trapped." From Eq. (9), by setting $\mathbf{v}_P = 0$, it is possible to determine the electrokinetic equilibrium condition (E_{EEC}) as:

$$\mu_{EO}\mathbf{E} + \mu_{EP}^{(1)}\mathbf{E} = -\mu_{EP}^{(3)}|\mathbf{E}|^3\mathbf{i} \tag{10}$$

$$E_{EEC} = \sqrt{-\frac{\left(\mu_{EP}^{(1)} + \mu_{EO}\right)}{\mu_{EP}^{(3)}}} \tag{11}$$

The present study aims to validate the applicability of the parameter E_{EEC} by conducting experiments in different insulator-based channel designs with biological samples; the value of E_{EEC} for each cell should be the same in all distinct insulator-based channel designs.

It is important to note that both $\mu_{EP}^{(1)}$ and $\mu_{EP}^{(3)}$ will always be negative for negatively charged particles (Fig. 1d). Therefore, E_{EEC} is a real number when μ_{EO} has a larger magnitude than $\mu_{EP}^{(1)}$, which is common for micron-sized particles, such as cells [43]. For the case of a positively charged particle (Fig. 1d) in a channel with a negative surface charge (negative ζ_W), there is no E_{EEC} as the particle will increase in velocity magnitude for a higher electric field and keep migrating toward the negative electrode. Detailed information on the 2D COMSOL mathematical model used to estimate the electric field distributions within our devices is included in the ESM file. For our study, a 2D model was selected, since for shallow channels like the ones employed here, there are no significant differences between the results obtained with 2D and 3D models [44]. Cardenas-Benitez et al. first proposed the use of the E_{EEC} in insulator-based channels [45].

Materials and methods

Microdevices

Two distinct insulator-based EK channel designs were fabricated from PDMS; both designs included an array of insulating posts (Fig. 1). Standard soft lithography techniques were followed to create a device from PDMS (Dow Corning, Midland, MI) molded on a silicon wafer (Silicon Inc., Boise, ID) that had been patterned using SU-83050 photoresist (MicroChem, Newton, MA). Once the PDMS slab cured at 85 °C for 40 min and 135 °C for 5 min, it was removed from the negative mold and the inlet/outlet reservoirs (2 mm diameter) were manually punched. To seal the channels, a plasma corona wand (Electro Technic Products, Chicago, IL) was utilized to activate the PDMS slab and the surface area of a glass wafer (4″ diameter) which was spin-coated with a thin layer of PDMS. This step ensures the internal channel surfaces are composed of PDMS and thus have the same zeta potential of the wall (ζ_W) and allow consistent *EO* flow through the channel. The dimensions of both microchannel designs were 10.16 mm long, 40 μm deep, and 880 μm wide, and the

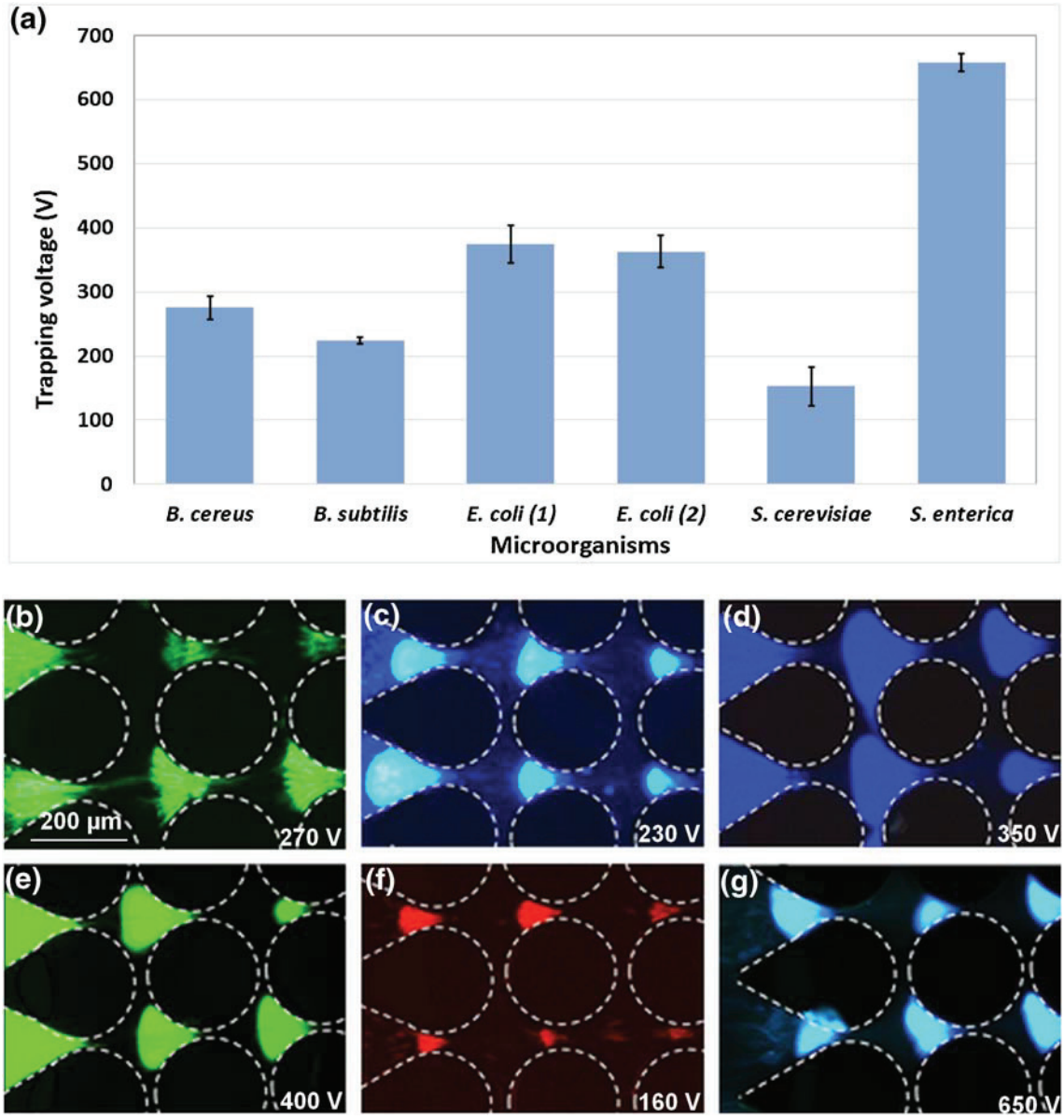

Fig. 2 Illustration of the trapping of all microorganisms in this study in circle-shaped posts devices. **a** Trapping voltage for each strain. Images of trapping for **b** *B. cereus* at 270 V, **c** *B. subtilis* at 230 V, **d** *E. coli* (1) at 350 V, **e** *E. coli* (2) at 400 V, **f** *S. cerevisiae* at 160 V, and **g** *S. enterica* at 650 V

specific parameters for the two post array geometries employed, circles and ovals, are included in Fig. 1.

Samples and suspending medium

The five different bacterial strains that were studied included *Bacillus subtilis* (ATCC® 6051™), *Bacillus cereus* (ATCC® 14579™), *Escherichia coli* (1) (ATCC® 11775™), *Escherichia coli* (2) (ATCC® 25922™), and *Salmonella enterica* serovar Typhimurium (TT9079). One strain of *Saccharomyces cerevisiae* (ATCC® 9763™) was also employed. Each microorganism was cultured in its respective liquid media (*B. cereus* and *B. subtilis* in TSB, *S. cerevisiae* in YMB, and *S. enterica* and *E. coli* in LB) and grown to an optical density (OD) that correlated with its respective exponential growth curve. After the OD was measured, the samples were stained following a standard labeling procedure with the Syto DNA-intercalating dyes [43]. The final sample was then suspended in DI water with a conductivity between 10 and 17 μS/cm and a pH between 6.8 and 7.5, which produced a ζ_W of approximately − 108.57 mV. DI water was also used to prefill the channels prior to conducting the experiments.

Equipment and software

Cell behavior was observed and recorded in the form of videos and pictures with a Leica DMi8 inverted microscope (Wetzlar, Germany) paired with a Leica DFC7000 T camera and the

software *LASX* provided by the manufacturer. A personal computer was required to operate the voltage sequencer and microscope. DC electric potentials were applied across the length of the channel by employing the high voltage supply (Model HVS6000D, LabSmith, Livermore, CA). The voltage sequencer was manipulated with the software *Sequence* provided by the manufacturer. COMSOL *Multiphysics*® 4.4 was used to estimate the magnitude of the electrokinetic equilibrium condition (E_{EEC}) value for each strain (Eq. (11)).

Experimental procedure

The experiments started by introducing a 2–20-μL sample of the selected microorganism to the inlet of the channel prefilled with DI water and placing platinum wire electrodes at the reservoirs in order to apply a DC potential across the channel length. Microorganism response was observed and recorded for each experiment. Rather than using the standard trapping voltage, at which particles are trapped with little to no observable particle leaking from the band of trapped particles, for the purpose of this study, a "sufficient" trapping voltage was determined. Sufficient trapping was defined as the required voltage to obtain a band or cluster of trapped bacterial or yeast particles that is sufficiently thick to be observed with minimal particle leakage. This was done to standardize the trapping voltage requirements of the different microorganisms despite the inherent population variability that exists among all living organisms (i.e., differences in size as they grow and reach their final size), which results in additional cell leaking. During the "sufficient" trapping experiments, the applied voltage was varied between 100 and 800 V in the circle-shaped post device and between 100 and 650 V in the oval-shaped post device until a distinct band could be observed and recorded as the sufficient trapping voltages. The results for the circle-shaped post devices are reported in Figs. 2 and 3 and ESM Table S2, which include the detailed trapping voltage data and estimated E_{EEC} for each strain, and the results for the oval-shaped post devices are reported in Fig. 4 and ESM Table S3, which include the detailed experimental and expected trapping voltage data for each strain, along with their respective relative errors.

Results and discussion

Experimental characterization of the electrokinetic trapping of microorganisms

The electrokinetic trapping of bacterial and yeast cells was explored through a series of experiments. The purpose was to determine the required voltage to "sufficiently" trap and enrich each type of organism in the device with circle-shaped insulating posts shown in Fig. 1a and b. After introducing the fluorescently labeled microorganism of interest into the channel, a voltage was applied, which was manually increased every 5 to 10 s, until the "sufficient" trapping of the organism was observed, as reported in Fig. 2a. The experiments were repeated at least three times for each organism to ensure the reproducibility of the results within the system. Figure 2b–g illustrate images of the trapping of all six organisms in the circle-shaped post device at applied potentials between 160 and 650 V.

As it can be observed in Fig. 2a, each strain tested had a distinct trapping voltage and strong reproducibility, as demonstrated by the small variation in trapping voltage. As expected, the two strains of *E. coli* yielded very similar values given that under DC potentials, the response of the organisms mainly depends on the cell membrane properties and the latter have nearly identical surface properties [39]. Moreover, the distinct trapping voltages yielded by the experiments support the potential of this system for applications differentiating distinct types of cells.

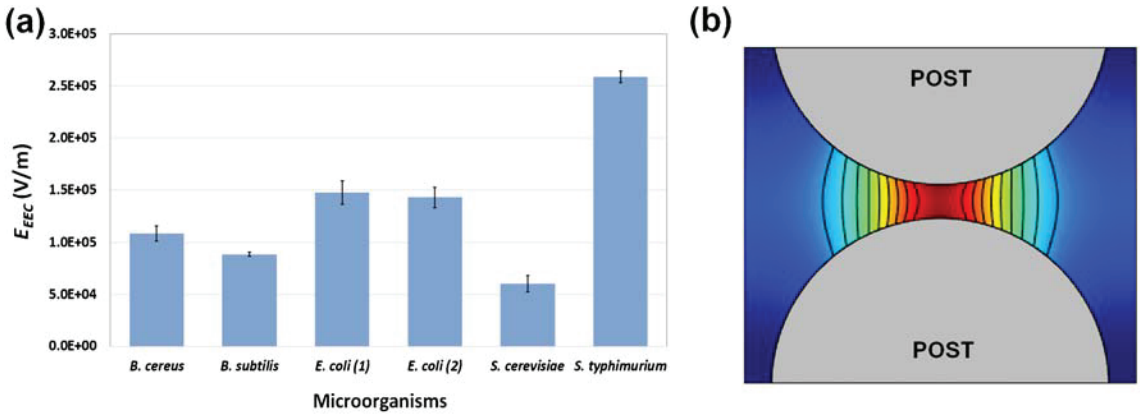

Fig. 3 Illustration of the E_{EEC} values and method of determination. **a** E_{EEC} values for each strain. **b** Plot of isometric lines of E_{EEC} between two posts. These can represent the E_{EEC} "signature" of a specific microorganism

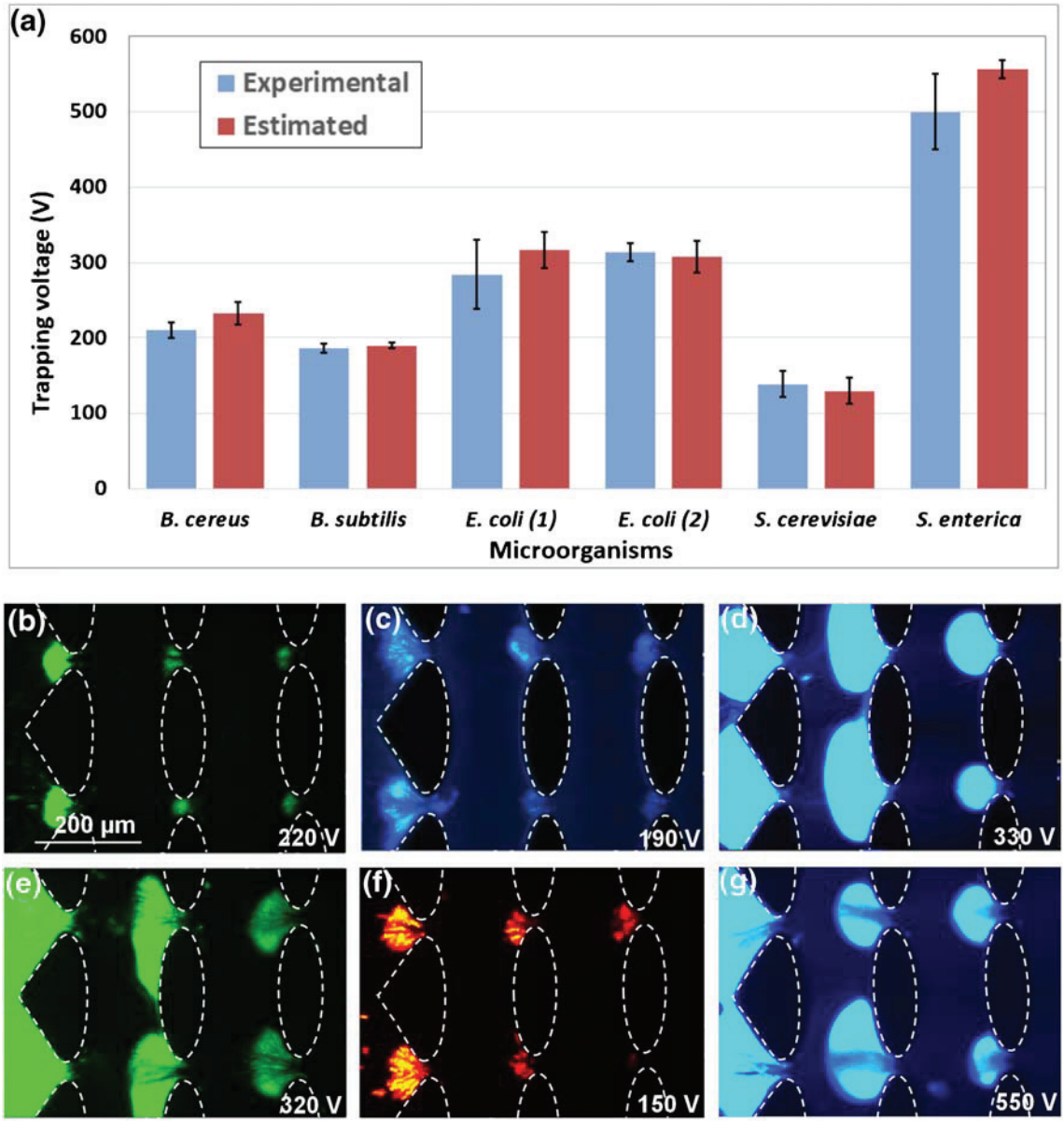

Fig. 4 Illustration of the trapping of all microorganisms in this study in oval-shaped post devices. **a** Comparison of the experimental and predicted trapping voltage for each strain. Images of trapping for **b** *B. cereus* at 220 V, **c** *B. subtilis* at 190 V, **d** *E. coli* (1) at 330 V, **e** *E. coli* (2) at 320 V, **f** *S. cerevisiae* at 150 V, and **g** *S. enterica* at 550 V

Modeling predictions for the trapping of bacteria and yeast

The trapping voltage (Fig. 2a) is useful for determining the applied potential at which a microorganism will stop migrating (becomes trapped) within a device allowing for significant enrichment. However, specific trapping voltage values obtained using the device with circle-shaped posts cannot be directly translated to a different channel design with different post geometries (e.g., oval posts in Fig. 1c). Normalizing the conditions at which particles and organisms are trapped in EK microscale devices has been explored by multiple research groups using the concept of trapping value (*Tv*) [15, 32, 33]. A newer research report considers the effects of electrophoresis of the second kind ($EP^{(3)}$) as one of the phenomena that causes particle trapping when particles are negatively charged as is the case with the bacterial and yeast species in this study (Fig. 1d). This new parameter is the electrokinetic equilibrium condition (E_{EEC}, Eq. (11)). The E_{EEC} of a particular cell type (Fig. 3a) should be transferable between any insulating post-based design since it considers both linear and non-linear electrokinetic effects acting on the cells. In order to determine the E_{EEC} of a particular cell type, the trapping voltage was experimentally determined and the electric field distribution within the entire device was simulated using COMSOL at the given trapping voltage. The electric field value at the center of

the constriction between two posts was considered to be equal to the E_{EEC} at the trapping voltage. The black lines in Fig. 3b depict the isometric curves within the constrictions obtained in a device with circle-shaped posts. The isometric curves act as a barrier, such that only cells with an E_{EEC} value higher than that of the isometric curve will pass through. This can be explained as the balance between the linear EK and $EP^{(3)}$ forces present in the system, which are opposite to each other. However, a particle with an E_{EEC} value equal or lower than that of the isometric curve will be stopped or driven back, as $EP^{(3)}$ will become the dominant effect within the constriction region.

Experimental validation of E_{EEC} library

To validate the results estimated using the COMSOL mathematical model, sufficient trapping experiments were repeated employing oval-shaped post devices (Fig. 1c). First, using the E_{EEC} values previously estimated for each strain (Fig. 3a and ESM Table S2) and integrating the oval-shaped post design into the mathematical model, we were able to estimate the required applied voltage to reach the E_{EEC} condition for each strain (Fig. 4a and ESM Table S3). Then, the sufficient trapping experiments were performed at least three times for each organism. The experimentally obtained trapping voltages are illustrated in Fig. 4a next to the predicted values. Figure 4b–g display images of the trapping of all six organisms in the oval-shaped post device at applied potentials between 150 and 550 V.

As it can be observed in Fig. 4a, each strain tested had a distinct trapping voltage and strong reproducibility, as demonstrated by the small variation in E_{EEC}. In addition, as shown graphically in Fig. 4a and listed in ESM Table S3, the COMSOL predictions were able to estimate the actual trapping voltages within a relative error of 2–12%. Furthermore, given the overlap between the error bars of our estimated and experimental values, it can be said this error is not statistically significant. Therefore, this low relative error is well within our tolerance and further proves the potential applicability of the EK library, in particular considering that biological organisms have an innate heterogeneity and that the effect of $\mathbf{v}_{DEP}$ was neglected as it only represents 0.89–5.85% of the total velocity of the particle (ESM Table S1).

Application: differentiation of two species of the same genus

This set of experiments aimed to differentiate two species of the same genus. As seen in Tables S2–S3 (see ESM), despite belonging to the same genus and having similar shapes and sizes, *B. subtilis* and *B. cereus* have different trapping voltages, 225 V and 276 V, respectively (Fig. 2a). This observation was further explored through a mixture separation experiment where *B. subtilis* and *B. cereus* were introduced into the device and exposed to voltages that would cause them to trap. As expected, given its lower "sufficient" trapping voltage, as seen in Fig. 5a, when an electric potential of 250 V was applied, only *B. subtilis* trapped, and as the voltage was increased to 300 V, *B. subtilis* was pushed back farther away from the constriction, while *B. cereus* trapped closer to the constriction, as seen in Fig. 5b. These findings illustrate the potential of employing experimental electrokinetic data for designing a separation process, which further emphasizes the need for an EK library with a wide number of microorganisms that is based on a parameter (E_{EEC}) which can be translated into different designs. An attractive feature of this technique is the sensitivity of the library as demonstrated by Fig. 5b where organisms of the same genus with a difference of 50 V in "sufficient" trapping voltage were differentiated into distinct bands. It should be noted that voltages slightly higher than the respective trapping voltages for each organism were used in this experiment for visualization purposes, in an attempt to increase the fluorescence within the constriction by slightly surpassing the "sufficient" trapping voltage.

Application: separation of three microorganisms of different sizes and shapes

After determining the different trapping voltages of each organism, a separation experiment was conducted with a sample containing *S. enterica*, *E. coli* (2), and *S. cerevisiae* cells. Figure 6a shows the trapping of all three cell types, where *S. enterica* (blue) is trapped at the center of the constriction, followed by *E. coli* (2) (green) and yeast cells (red) trapped at the wider region of the construction. The results in Fig. 6a, depicting distinct "trapping bands" for each microorganism, open the possibility for an electrokinetic-based separation. A sample containing all three cell types at a 1:1:1 ratio was injected into a microchannel with circle-shaped posts, and a voltage high enough to ensure the trapping of all three organisms was applied (900 V) for 15 s. The voltage was lowered to selectively release one type of microorganism at a time, as shown in Fig. 6b. Video footage was captured at the beginning of the post array as the strains were released and the signal was analyzed using the ImageJ software. To avoid capturing the signal from the trapping bands, five different interrogation windows were selected, from which the data was to be drawn. The fluorescence signal was measured from the video file (see ESM Video S1) using ImageJ, and the signal was adjusted with respect to the greatest fluorescence value yielded throughout the data. These normalized fluorescence values were then plotted against time (Fig. 6b). While it is difficult to differentiate between *S. enterica* (blue) and *E. coli* (2) (green) in the video, based on their respective trapping voltages, it was assumed that the first peak in Fig. 6b illustrates the

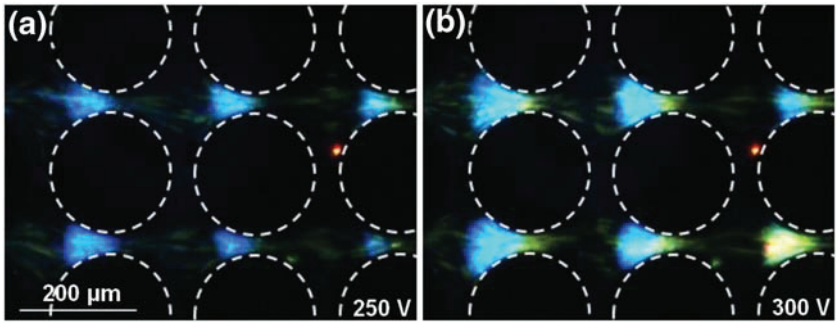

Fig. 5 Representation of the differential trapping behavior of two species from the same genus. **a** *B. subtilis* (blue), which has the lower trapping voltage, first traps at 250 V. **b** *B. cereus* (green), traps at 300 V, as expected from "sufficient" trapping voltage data

release of *S. enterica*, the second peak the release of *E. coli* (2), and the third peak the release of *S. cerevisiae* (red/orange). It must be noted, however, that these are biological samples, and as such, some variability in cell size is expected. Moreover, this variability in cell size can lead to some cross-contamination at a significantly lower concentration in the peaks. These promising results suggest the library can be used to characterize non-homogeneous mixtures of microorganisms as well as differentiate and potentially purify microorganisms using microscale electrokinetic devices.

Concluding remarks

The present contribution studies the EK behavior of six different microorganisms, including one yeast strain and five bacterial strains. Among the bacterial strains, two were of the same genus and two were strains of the same species. Insulator-based EK microdevices made from PDMS and containing arrays of insulating posts of two distinct shapes (circles and ovals) were employed. Experimental and mathematical analyses were carried out considering the effects of three *EK* phenomena: $EP^{(1)}$, $EP^{(3)}$, and *EO*. Dielectrophoretic effects were neglected since they have a small contribution to the overall particle behavior. The novel parameter of electrokinetic equilibrium condition (E_{EEC}) was employed to create a library of the *EK* signature for each strain. Furthermore, E_{EEC} was then used to extrapolate the conditions required for trapping a particular strain across distinct post designs, in this particular case from circle-shaped posts to oval-shaped posts. The results were very encouraging with excellent agreement between the predicted and the experimental E_{EEC} for all cells used. Moreover, while more work needs to be done to expand on use of the EK library, the small error ($\leq 12\%$) with which we were able to predict the trapping voltage in a different geometry is a promising first step toward validating this technique.

In addition to validating the applicability of the *EK* library, two distinct applications were carried out to support the sensitivity of the technique. The first application was the differentiation of cells from two distinct species (*B. cereus* and *B. subtilis*) of the same genus, an assessment of great biological significance as separations between organisms that grow in the same conditions and have similar membrane properties (Gram positive) are generally more intricate. The second application consisted of the simultaneous differentiation and characterization of a sample containing three distinct strains (*S. enterica*, *E. coli* (2), and *S. cerevisiae*). A voltage was applied to trap all strains followed by the selective release of enriched cells one strain at a time. The *EK* separation yielded the three distinct peaks, which further supports the potential applications of an E_{EEC}-based *EK* library by suggesting this

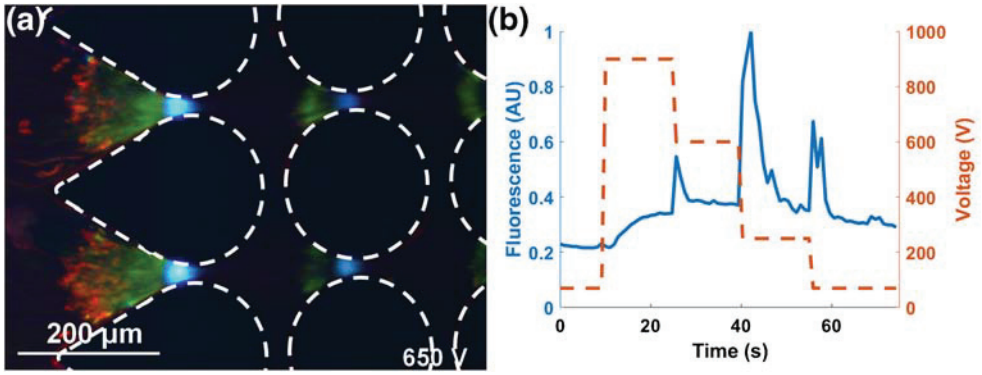

Fig. 6 Illustration of simultaneous analysis and separation by controlled release of three distinct microorganisms; *S. cerevisiae* in orange/red, *E. coli* (2) in green, and *S. enterica* in blue. **a** Image showing the three organisms trapping at 650 V in the order predicted by their individual trapping voltages. **b** Electrokinetic separation showing the release of *S. enterica*, *E. coli* (2), and *S. cerevisiae*, in that order, as peaks of enriched cells

approach can be used not only for the rapid analysis of heterogeneous bacterial or yeast samples but also to purify them.

Acknowledgments The authors would like to thank Dr. Julie Thomas from the Rochester Institute of Technology for the *S. enterica* strain used in this study.

Funding information The authors received financial support from the National Science Foundation (CBET- 1705895). AOH and AP received support from the National Institutes of Health (NIH) award R15GM120653, and ongoing support from the College of Science and the Thomas H. Gosnell School of Life Sciences.

Compliance with ethical standards

Conflict of interest The authors declare that they have no competing interests.

Ethical approval This article does not contain any studies with human participants or animals.

Informed consent Informed consent is not applicable in this study.

References

1. Schloss PD, Handelsman J. Status of the microbial census. Microbiol Mol Biol Rev. 2004;68(4):686–91.
2. Dykhuizen D. Species numbers in bacteria. Proc Calif Acad Sci. 2005;56(6 Suppl 1):62–71.
3. Rampelotto PH. Extremophiles and extreme environments. Life. 2013;3(3):482–5.
4. Váradi L, Luo JL, Hibbs DE, Perry JD, Anderson RJ, Orenga S, et al. Methods for the detection and identification of pathogenic bacteria: past, present, and future. Chem Soc Rev. 2017;46(16):4818–32.
5. Land GA, Vinton EC, Adcock GB, Hopkins JM. Improved auxanographic method for yeast assimilations: a comparison with other approaches. J Clin Microbiol. 1975;2(3):206–17.
6. Whitesides GM. The origins and the future of microfluidics. Nature. 2006;442(7101):368–73.
7. Lapizco-Encinas BH. Chapter 7 Applications of dielectrophoresis in microfluidics. Microfluidics in detection science: lab-on-a-chip technologies. Cambridge: The Royal Society of Chemistry; 2015. p. 192–223.
8. Kirby BJ. Micro- and nanoscale fluid mechanics. Transport in microfluidic devices. New York: Cambridge University Press; 2010.
9. Sonnenberg A, Marciniak JY, McCanna J, Krishnan R, Rassenti L, Kipps TJ, et al. Dielectrophoretic isolation and detection of cfc-DNA nanoparticulate biomarkers and virus from blood. Electrophoresis. 2013;34(7):1076–84.
10. Abd Rahman N, Ibrahim F, Yafouz B. Dielectrophoresis for biomedical sciences applications: a review. Sensors. 2017;17(3):449.
11. Douglas TA, Cemazar J, Balani N, Sweeney DC, Schmelz EM, Davalos RV. A feasibility study for enrichment of highly aggressive cancer subpopulations by their biophysical properties via dielectrophoresis enhanced with synergistic fluid flow. Electrophoresis. 2017;38(11):1507–14.
12. Nakano A, Camacho-Alanis F, Ros A. Insulator-based dielectrophoresis with [small beta]-galactosidase in nanostructured devices. Analyst. 2015;140(3):860–8.
13. Ai Y, Zeng Z, Qian S. Direct numerical simulation of AC dielectrophoretic particle–particle interactive motions. J Colloid Interface Sci. 2014;417:72–9.
14. LaLonde A, Romero-Creel MF, Lapizco-Encinas BH. Assessment of cell viability after manipulation with insulator-based dielectrophoresis. Electrophoresis. 2015;36(13):1479–84.
15. Coll De Peña A, Mohd Redzuan NH, Abajorga M, Thomas JA, Lapizco-Encinas BH. On the potential analysis of bacteriophage viruses with insulator-based dielectrophoresis. Micromachines. 2019;10(7):450.
16. Adekanmbi EO, Srivastava SK. Dielectrophoretic applications for disease diagnostics using lab-on-a-chip platforms. Lab Chip. 2016;16(12):2148–67.
17. Jones PV, Salmon GL, Ros A. Continuous separation of DNA molecules by size using insulator-based dielectrophoresis. Anal Chem. 2017;89(3):1531–9.
18. Szumski M, Klodzinska E, Buszewski B. Separation of microorganisms using electromigration techniques. J Chromatogr A. 2005;1084(1–2):186–93.
19. Pethig R. Review—where is dielectrophoresis (DEP) going? J Electrochem Soc. 2017;164(5):B3049–B55.
20. Lapizco-Encinas BH. On the recent developments of insulator-based dielectrophoresis: a review. Electrophoresis. 2019;40(3):358–75.
21. Xuan X. Recent advances in direct current electrokinetic manipulation of particles for microfluidic applications. Electrophoresis. 2019;40(18–19):2484–513.
22. Romero-Creel M, Goodrich E, Polniak D, Lapizco-Encinas B. Assessment of sub-micron particles by exploiting charge differences with dielectrophoresis. Micromachines. 2017;8(8):239–53.
23. Dukhin SS. Electrokinetic phenomena of the second kind and their applications. Adv Colloid Interf Sci. 1991;35:173–96.
24. Schnitzer O, Zeyde R, Yavneh I, Yariv E. Weakly nonlinear electrophoresis of a highly charged colloidal particle. Phys Fluids. 2013;25(5):052004.
25. Figliuzzi B, Chan WHR, Moran JL, Buie CR. Nonlinear electrophoresis of ideally polarizable particles. Phys Fluids. 2014;26(10):102002.
26. Schnitzer O, Yariv E. Nonlinear electrophoresis at arbitrary field strengths: small-Dukhin-number analysis. Phys Fluids. 2014;26(12):122002.
27. Khair AS. Strong deformation of the thick electric double layer around a charged particle during sedimentation or electrophoresis. Langmuir. 2018;34(3):876–85.
28. Elitas M, Dhar N, Schneider K, Valero A, Braschler T, McKinney JD, et al. Dielectrophoresis as a single cell characterization method for bacteria. Biomed Phys Eng Express. 2017;3(1):015005.
29. Hilton SH, Hayes MA. A mathematical model of dielectrophoretic data to connect measurements with cell properties. Anal Bioanal Chem. 2019;411:2223–2237. https://doi.org/10.1007/s00216-019-01757-7.
30. Syed LU, Liu J, Price AK, Li Y-f, Culbertson CT, Li J. Dielectrophoretic capture of E. coli cells at micropatterned nanoelectrode arrays. Electrophoresis. 2011;32(17):2358–65.
31. Seyedi SS, Matyushov DV. Protein dielectrophoresis in solution. J Phys Chem B. 2018;122(39):9119–27.
32. Mohammadi M, Zare MJ, Madadi H, Sellarès J, Casals-Terré J. A new approach to design an efficient micropost array for enhanced direct-current insulator-based dielectrophoretic trapping. Anal Bioanal Chem. 2016;408(19):5285–94.
33. Crowther CV, Hayes MA. Refinement of insulator-based dielectrophoresis. Analyst. 2017;142(9):1608–18.
34. Wang Q, Jones AAD 3rd, Gralnick JA, Lin L, Buie CR. Microfluidic dielectrophoresis illuminates the relationship between microbial cell envelope polarizability and electrochemical activity. Sci Adv. 2019;5(1):eaat5664–eaat.

35. Betts WB. The potential of dielectrophoresis for the real-time detection of microorganisms in foods. Trends Food Sci Technol. 1995;6(2):51–8.
36. Markx GH, Dyda PA, Pethig R. Dielectrophoretic separation of bacteria using a conductivity gradient. J Biotechnol. 1996;51(2):175–80.
37. Suehiro J, Noutomi D, Shutou M, Hara M. Selective detection of specific bacteria using dielectrophoretic impedance measurement method combined with an antigen-antibody reaction. J Electrost. 2003;58(3/4):229–46.
38. Bennett D, Khusid B, James C, Galambos P, Okandan M, Jacqmin D, et al. Combined field-induced dielectrophoresis and phase separation for manipulating particles in microfluidics. Appl Phys Lett. 2003;83(23):4866–8.
39. Lapizco-Encinas BH, Simmons BA, Cummings EB, Fintschenko Y. Dielectrophoretic concentration and separation of live and dead bacteria in an array of insulators. Anal Chem. 2004;76(6):1571–9.
40. Lapizco-Encinas BH, Davalos R, Simmons BA, Cummings EB, Fintschenko Y. An insulator-based (electrodeless) dielectrophoretic concentrator for microbes in water. J Microbiol Methods. 2005;62:317–26.
41. Probstein RF. Physicochemical hydrodynamics: an introduction. Wiley; 2005.
42. Shilov V, Barany S, Grosse C, Shramko O. Field-induced disturbance of the double layer electro-neutrality and non-linear electrophoresis. Adv Colloid Interf Sci. 2003;104(1):159–73.
43. Saucedo-Espinosa MA, LaLonde A, Gencoglu A, Romero-Creel MF, Dolas JR, Lapizco-Encinas BH. Dielectrophoretic manipulation of particle mixtures employing asymmetric insulating posts. Electrophoresis. 2016;37(2):282–90.
44. Baylon-Cardiel JL, Lapizco-Encinas BH, Reyes-Betanzo C, Chávez-Santoscoy AV, Martínez Chapa SO. Prediction of trapping zones in an insulator-based dielectrophoretic device. Lab Chip. 2009;9(20):2896–901.
45. Cardenas-Benitez B, Lapizco-Encinas BH, Jind B, Gallo-Villanueva RC, Martinez-Chapa SO, Perez-Gonzalez VH. Direct current electrokinetic particle trapping in insulator-based microfluidics: theory and experiments. Submitted, 2020.